

Unconventional Methods For Unconventional Plays:

Using Elemental Data To Understand Shale Resource Plays

Ken Ratcliffe and Milly Wright, Chemostrat; Dave Spain, BP USA

Part 2

Introduction

In the last edition of *PESA News Resources* (No 116), the use of chemostratigraphy to help refine stratigraphic understanding of shale resource plays was discussed. Following on from Part 1, we will here look at what additional information can be gathered about shale reservoirs from the same elemental dataset that provides chemostratigraphic correlations.

Mineral modelling in the Haynesville formation

An important aspect to understanding shale reservoirs is determining their mineralogy and TOC (total organic carbon) content, since these will essentially control reservoir quality. Typically, this is achieved using X-Ray diffraction (XRD) and LECO TOC analysis respectively. XRD, in particular, is expensive and results can take a considerable time to acquire. From Figure 1, however, it is clear that a close relationship exists between major elements and common rock forming minerals. This relationship is to be expected, since the primary control on whole rock inorganic geochemical data is the component mineralogy

(Pearce et al., 2005, Ratcliffe et al., 2010), but it also forms the basis for calculating mineralogical compositions from elemental data. Simplistically, where an R^2 value between a mineral and an element exceeds 0.8, the linear regression between the two can be used to model mineral abundances. For example on Figure 1A, the regression equation $y=0.47x+2.97$ (where y is the concentration of Al_2O_3 [known] and x is the amount of illite [unknown]) can be used to determine illite abundances in samples where Al_2O_3 concentrations have been determined, but where XRD data have not been acquired. However, the regression lines are formation specific and more often than not, the relationship is more complex than a simple high R^2 linear relationship. There are several public domain software packages that exist for automatically calculating mineralogy from geochemistry (ModAn, Sednorm and Minlith) (Paktunc, 2001, Rosen et al., 2004), which form the basis for in-house algorithms used by Chemostrat. Figure 2 displays a comparison of directly measured mineralogy obtained by XRD analyses and calculated mineralogy, using an in-house mineral modelling. It is clear that for most of the common minerals, the calculated mineralogy closely matches the directly measured mineralogy. While this method may not be able to determine

more subtle mineralogical variations, such as the illite-smectite abundances, it does provide a reasonable indication of bulk mineralogy and this is achieved quickly and inexpensively from the dataset that has been obtained primarily for stratigraphic correlations.

In addition to mineralogy, it is possible to approximate TOC levels using geochemical data. Figure 1E shows the relationship between Mo concentrations and TOC values. When samples with over 10 ppm Mo are removed, the two variables have an R^2 values of 0.88, i.e. a highly significant relationship. The samples with Mo values greater than 10 ppm also have high values of Ni and V, which suggests that the high Mo in these samples are associated with minerals derived from authigenic enrichment under anoxic conditions (sensu Tribouillard et al., 2006, see discussion below), rather than a direct relationship to organic carbon. Using the regression equation shown on Figure 2E ($TOC_{calc} = 0.3325 * Mo + 0.3108$), the TOC_{calc} values shown on Figure 2 are generated. Apart from samples with Mo >10 ppm, there is a close correspondence between $TOC_{measured}$ and TOC_{calc} . This may not be as precise as direct measurement of TOC using LECO, but it provides a quick and inexpensive reasonable approximation of TOC.

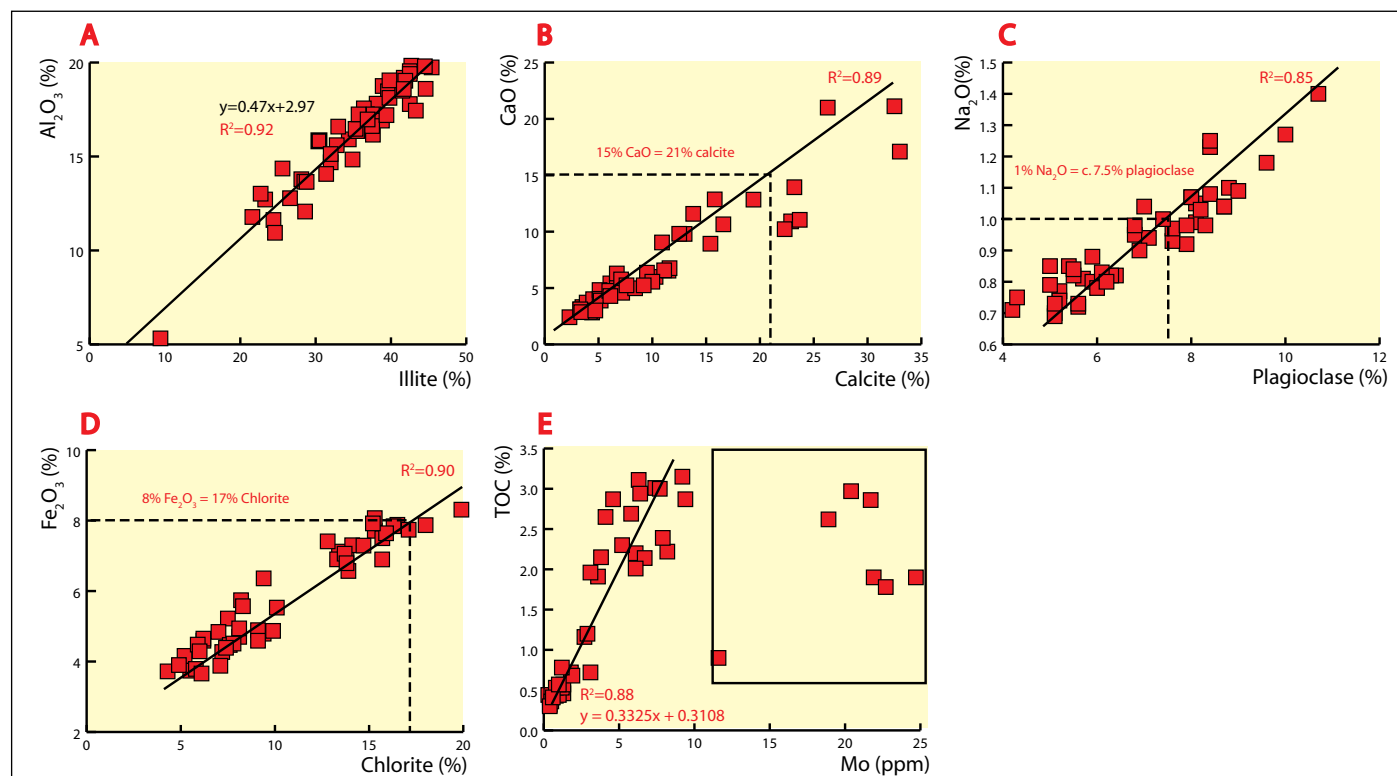


Figure 1. 1A-D: Cross plots of selected elements and minerals, with regression coefficient (R^2) displayed. Mineral data were acquired using XRD. 1E: Cross-plot of Mo and TOC values, with R^2 and regression line equation displayed. TOC values obtained from LECO analysis. All ICP, XRD and LECO TOC analyses were carried out on a subsample of homogenised powder.

Paleoredox modelling in the Haynesville formation

Understanding paleoredox conditions is of paramount importance to shale gas exploration because high TOC values are typically found in sediments deposited where bottom water condition were anoxic. Oceanic anoxic events have long been recognised and studied (Schlanger and Jenkyns, 1976) and in recent years, much has been written on the use of elemental geochemistry in sediments and water columns as a proxy for depositional redox conditions (e.g. Tribovillard et al., 2006, Turgen and Brumsack, 2006, Tribovillard et al., 2008, Negri et al., 2009, Jenkyns, 2010).

As demonstrated in Part 1 of this article, a group of elements (Mo, U, Ni, V, Cu, Zn and Co) all plot in close proximity to one another on a cross plot of Eigen vector 1 vs Eigen vector 2, implying that they are all somehow relate to one another within the sediments. These elements are typically associated with authigenic enrichment within the sediment under anoxic conditions (Tribovillard et al., 2006) and as such are potentially important indicators of anoxia.

When dealing with element enrichments, the level of enrichment is typically expressed by comparison against “standard marine” shales. These are referred to as enrichment factors (EF) and are calculated as follows (Tribovillard et al., 2006): $ElementEF = (Element_{sample} / Al_2O_{3sample}) / (Element_{SMS} / Al_2O_{3SMS})$, where EF = enrichment factor, SMS = standard marine shale (SMS values taken from Tribovillard et al., 2006). Once calculated, EF values of 1 indicate no enrichment of an element relative to a standard marine shale that was deposited in oxic conditions, whereas values significantly greater than 1 imply the element has been enriched although the mechanism for that enrichment will vary. Figure

3 shows that within parts of the Haynesville formation, EF far in excess of 1 are seen for Mo, U, Ni and V, all elements that becomes authigenically enriched in sediments deposited under anoxic conditions. Figure 3 also demonstrates in that EF's in Package 4 are all low, implying conditions where oxic to suboxic during the deposition of the Bossier formation, whereas EF values in Package 2 are >1 implying anoxic conditions during deposition of the Haynesville formation, with notably high values recorded toward the bottom of Package 2 (unit 2.1).

Watson-4 and Gasplie Ocie-10, EF values are lower in Package 2 than they are in Johnston Trust-1-2H and Elm Grove Plantation, implying lateral changes in anoxia. Figure 4 displays the lateral variations in average EF of vanadium for the entire Haynesville formation (Chemostratigraphic Package 2) in all study wells. It is apparent from this figure that during deposition of the Haynesville formation there was greater authigenic enrichment of V in the eastern parts of the basin than in the westerly areas. This implies that there was greater anoxia in the east and therefore greater potential for organic matter preservation.

From Figure 3 it is also apparent that in wells

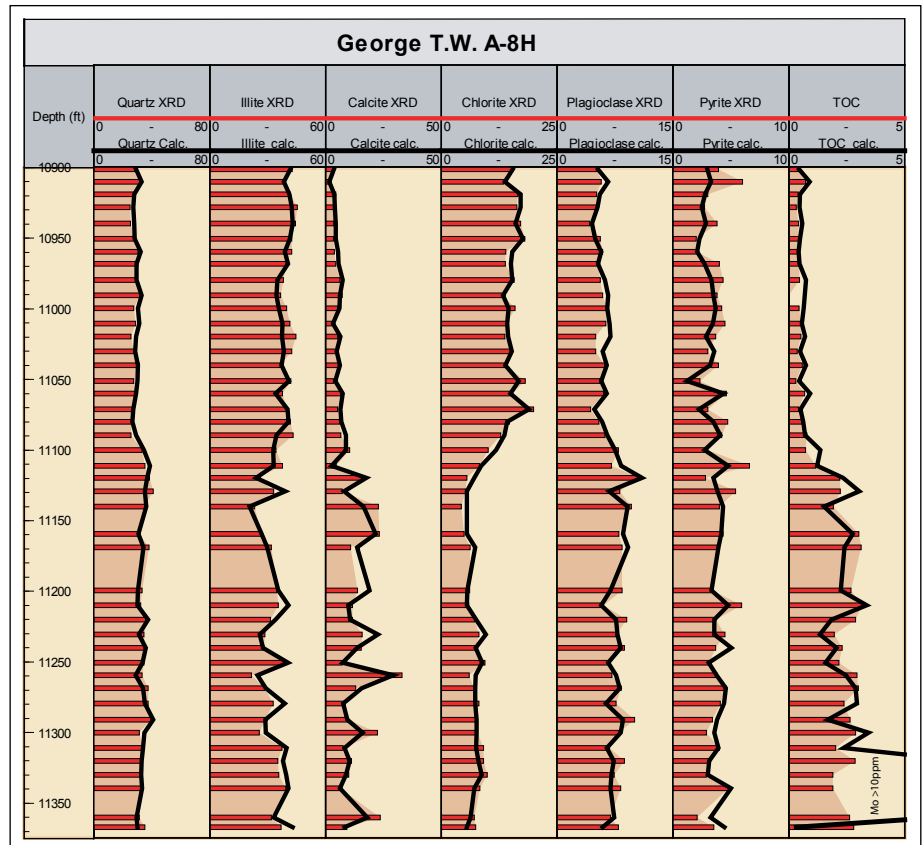


Figure 2. Vertical distribution of minerals in well George T.W. A-8H. Bar charts are data derived from XRD and LECO TOC analyses. Line graphs are mineral data calculated from elemental data.

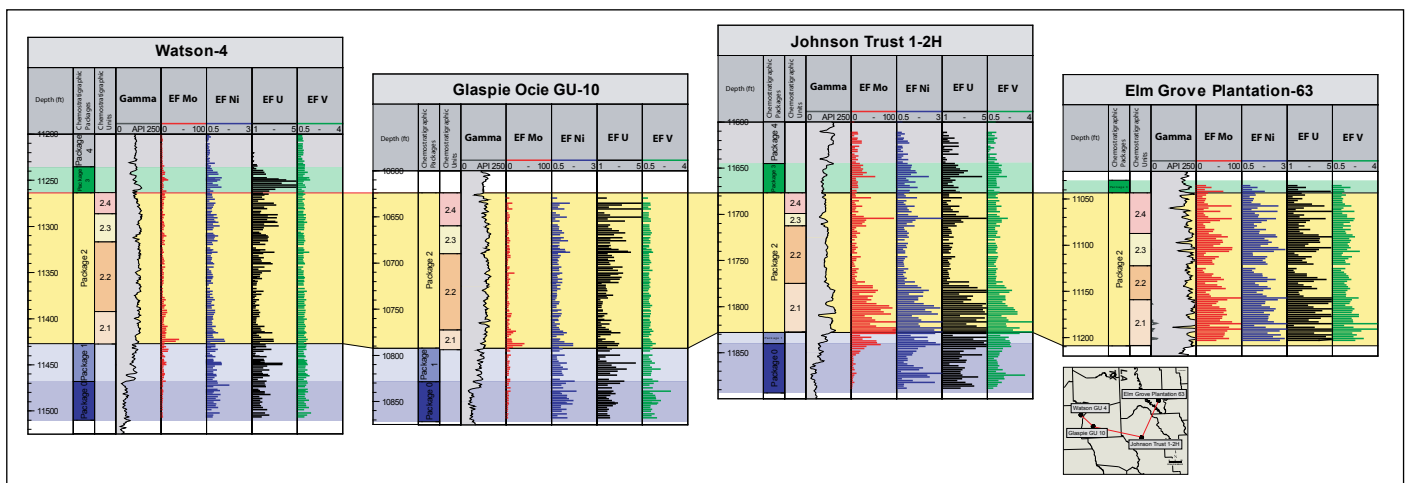


Figure 3. Selected element enrichment factors (EF) for wells Watson-4, Gasplie Ocie GU-10, Elm Grove Plantation-63 and Johnson Trust 1-2H. (The inset map shows the position of these wells). EF's for U(ppm), V(ppm), Mo(ppm) and Ni(ppm) have been the plotted for the study intervals in these wells, with Package 2 (the chemically defined Haynesville formation) correlated for stratigraphic context.

Recognition and application of changes in terrigenous input

As demonstrated in the preceding section, the elemental geochemistry of the Haynesville formation is to a large extent controlled by authigenic enrichment from sea water. However, there is undoubtedly a component of the geochemistry that is associated with land-derived debris. The amount of terrigenous input can be modelled from the major element geochemistry by combining those major elements associated with Group 3 on the Eigen vector plot presented in Part 1 (Figure 5 Part 1) of this article. On Figure 5, terrestrial input is calculated by summing Al_2O_3 , TiO_2 , Na_2O and K_2O values; SiO_2 is not incorporated in this summation, since it can also be associated with biogenic quartz (see succeeding discussion). When terrigenous content is plotted against depth, it is apparent that there is a gradual increase from local minima at the base of the Haynesville / Smackover transition (Package 1) to a maximum value $2/3$ of the way through Package 2 (=Haynesville formation). From this point, the terrigenous content remains high within Package 2, decreasing into Package 3 and increasing again sharply at the base of Package 4 (=the Bossier formation [not shown]). These long-term trends in terrigenous content are interpreted to reflect the proximity of the paleoshoreline; high terrigenous content occurs when the paleoshoreline extends into the basin, i.e. during lowstand periods and low terrigenous contents are found when the shoreline has been pushed landward by high base level. The long term changes in terrigenous contents seen in Figure 5 are therefore considered to reflect 1st order sea level fluctuations.

Superimposed on these 1st order variations defined by terrigenous content are a series of shorter-term cyclical changes in Zr/Nb and SiO_2/Al_2O_3 values (Figure 5). The SiO_2/Al_2O_3 and Zr/Nb chemical logs display notable similarities on Figure 5, suggesting they are both controlled by the same processes. SiO_2/Al_2O_3 typically reflects the abundance of silt-grade quartz in sediments and as such is normally a reliable grain size indicator. However, as discussed below, SiO_2 can also be associated with biogenic quartz in shale gas plays. The similarity of Zr/Nb chemical logs to SiO_2/Al_2O_3 logs in the Haynesville suggests it could provide be a proxy for grain size. Zr is normally associated with detrital zircon in sediments, while Nb is often associated with clay minerals, typically illite. Therefore, the Zr/Nb ratio is a good grain size indicator that is free from influence of biogenic silica.

Typically, an upward coarsening interval is used to define an upward shoaling sequence, terminating in a maximum regressive surface (MRS) and an upward fining interval is used to

define a transgressive sequence, culminating in a maximum flooding surface (MFS) (Donovan, 2010, Embry, 2010 and references cited therein). Therefore, the highest values of Zr/Nb (=coarsest sediment) correspond to an MRS and lowest values to a MFS. Figure 5 displays the resultant correlation between select wells when MRSs

and MFSs are defined using Zr/Nb values. The correlation on Figure 5 implies that regressive portions of the cycles are better developed in the west than in the east, where terrigenous content is high. Transgressive portions of the cycles are better developed in the east where terrigenous content is low, but organic content is high and

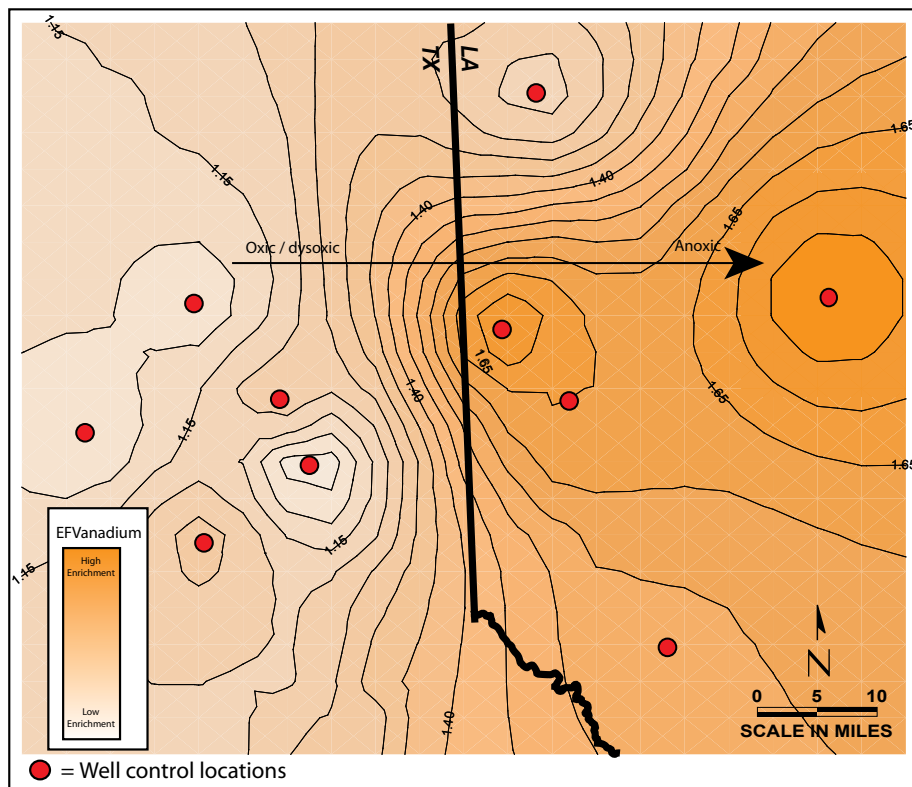


Figure 4. Map showing the average values for the enrichment factor of vanadium (EFV). Darker shading represents a higher average EFV value for the Haynesville formation (Package 2). Red circles mark points of well control in the area used to build this map. Additionally, the Louisiana/Texas border has been superimposed for geographic context.

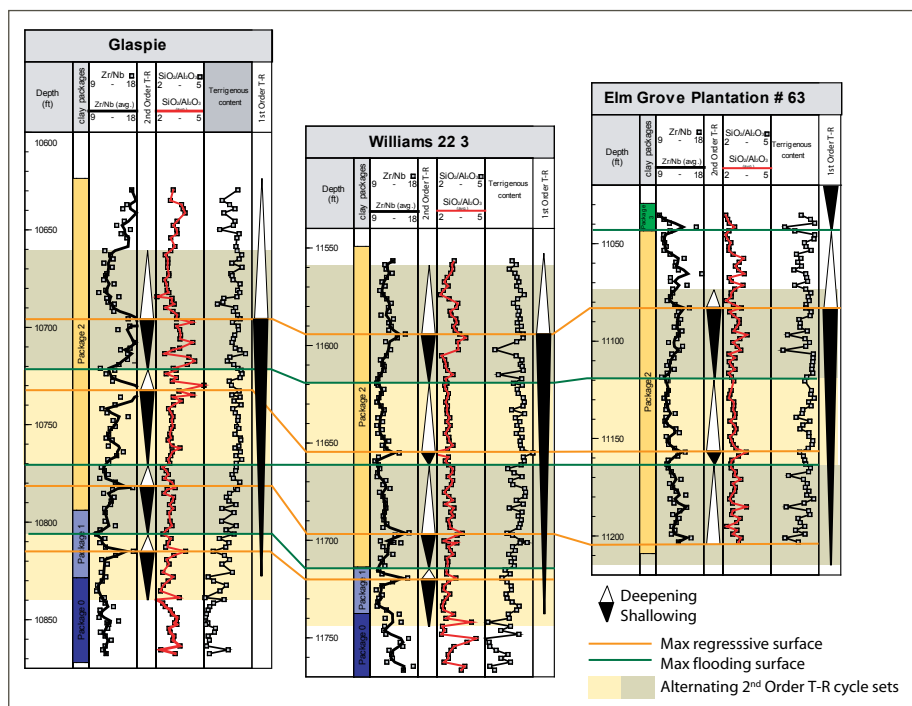


Figure 5. Terrigenous content, SiO_2/Al_2O_3 and Zr/Nb chemical logs plotted for selected wells to highlight long term (1st Order) and shorter term (2nd Order) cyclical fluctuations in the geochemical data.

shale exploration

anoxia was most severe. It also suggests that at least one regressive cycle is absent, or much thinned in the east of the basin.

Recognition of zones containing biogenic silica

As mentioned above, SiO_2 is not used in terrigenous input calculations. This is because some shale gas reservoirs such as the Muskwa and the Woodford formations contain high biogenic quartz contents. Recognition of zones with high biogenic quartz is critical to reservoir quality in shales effecting porosity, brittleness and log response. Although the amount of biogenic quartz cannot be quantified using whole rock geochemical data, samples that contain a significant component of biogenic silica can be identified from geochemical data using relative proportions of SiO_2 and Zr (Figure 6). SiO_2 is proportional to the amount of quartz in the shale and Zr is associated with the heavy mineral zircon. Zircon represents a proxy for all silt-sized terrestrial input and, as such, displays a linear association with detrital quartz (terrestrial trend on Figure 6). However, in samples where SiO_2 increases, but Zr decreases, i.e. a negative trend between quartz and terrestrial input, it can be implied that biogenic rather than detrital quartz is providing the SiO_2 (biogenic trend on Figure 6). Haynesville formation samples all plot with a terrestrial trend, implying that biogenic quartz is not present in the Haynesville formation. However a significant number of samples from the Muskwa formation plot on the biogenic trend, indicating samples from that formation that contain a significant portion of biogenic quartz.

Comparison of the Haynesville formation and the Eagle Ford formation

Most of the discussions in Part 2 of this article have concentrated on the Haynesville formation. Figure 7 uses a series of binary diagrams to highlight that not all shales are the same.

Figures 7a and 7b show that the Haynesville formation has generally higher $\text{Si}_2\text{O}/\text{Al}_2\text{O}_3$ values than the Eagle Ford formation, suggesting that it is relatively quartz-rich. Figure 7c shows a clear positive linear relationship between Zr and SiO_2 , indicating that the quartz from both the Haynesville formation and the Eagle Ford formation is dominantly detrital in origin.

Figure 7b also demonstrates that overall the Eagle Ford formation contains more CaO, implying it is a more calcareous shale. XRD data reveal that average calcite in the Eagle Ford formation is 33% (unpublished data) and is 10% in the Haynesville formation.

Figure 7d demonstrates that, largely, the Haynesville formation has higher Na_2O values than the Eagle Ford formation, which implies that it contains more plagioclase feldspar. XRD data reveal that average plagioclase content of the Eagle Ford formation is 1% (unpublished data) and is 7% in the Haynesville formation, supporting the assumption made from the elemental data.

Figure 7e demonstrates that the Haynesville formation has generally higher Fe_2O_3 values than the Eagle Ford formation, which implies it contains more chlorite. XRD data reveal that average chlorite content of the Eagle Ford formation is 4% (unpublished data) and is 7% in the Haynesville formation, supporting the assumption made from the elemental data.

Figure 7f shows that in the Haynesville formation there is a broad linear relationship between Al_2O_3 and V in samples where V is less than 120 ppm, which implies that the V is associated with terrestrial input. However, the Haynesville formation samples with V values over 120 ppm show no linear association with Al_2O_3 , implying that the high V values reflect authigenic enrichment in anoxic conditions. V values in the Eagle Ford formation are generally above 120 ppm and do not display any linear relationship with Al_2O_3 , which implies that the V values in the Eagle Ford are almost solely associated with authigenic enrichment in anoxic conditions.

Conclusions

In Parts 1 and 2 of this article, it has been shown that the 50 element data set acquired when carrying out chemostratigraphy on shales provides:

1. A means to devise regional stratigraphic frameworks that can be used for basin modelling;
2. A means to devise local, high resolution characterisations that can be used to determine well-bore

3. Recognition of coarsening and fining upward sequences which in some basins (such as the Haynesville-Bossier) may be interpreted in the context of transgressive and regressive cycles within a sequence stratigraphic model;
4. A means to quickly model bulk mineralogy;
5. A means to quickly model TOC contents;
6. Recognition of zones that contain biogenic silica; and
7. A means to model the relative degree of anoxia at the time of sediment deposition.

By providing all these lines of information from a single, relatively inexpensive, rapidly acquired dataset (including data capture at well-site), the whole rock geochemical data are shown to be a highly versatile and cost effective tool for the exploration, development and production of shale resource plays. Although we also highlight differences between shale formations here, with careful calibration and data manipulation, the applications demonstrated here can be readily exported to any shale resource play, of any age from around the world.

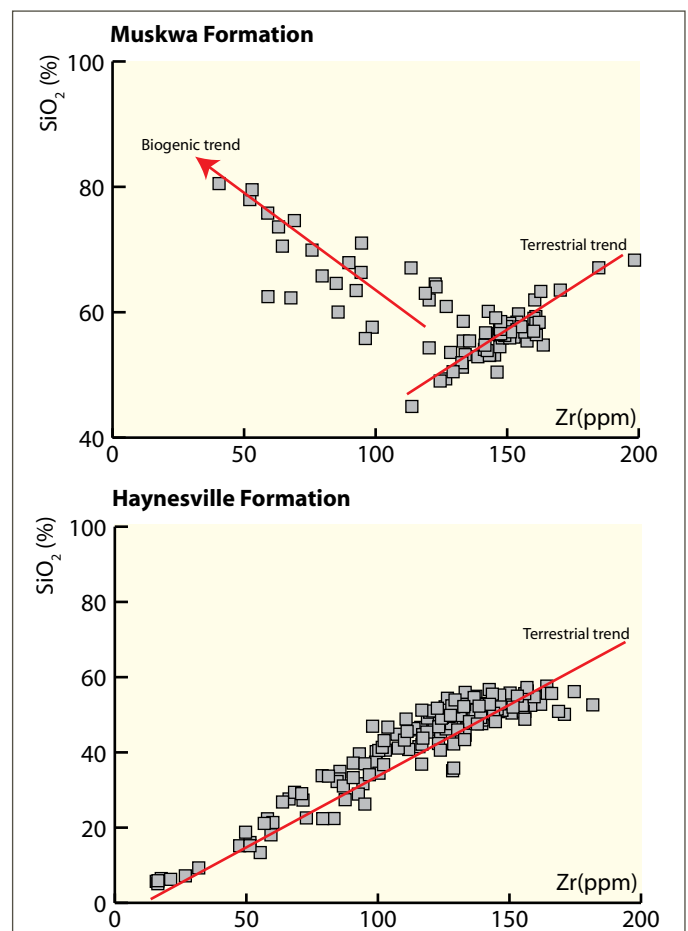


Figure 6. Zr vs. SiO_2 binary plots for data from the Muskwa and Haynesville formation. The positive linear trend line is termed the "terrestrial trend" and refers to samples where SiO_2 is derived from a terrestrial source. The negative linear trend line is termed the "biogenic trend" and refers to samples where a significant amount SiO_2 is derived from biogenic sources.

Acknowledgements

The authors would like to extend our gratitude to David Wray and Lorna Dyer of The University of Greenwich at Medway in the UK for preparing and analysing the samples on the ICP OES and MS. We would like to thank BP for its support and input throughout this study and for allowing data from wells Watson-4, Glaspie Ocie GU-10, George T.W. GUA-8H and CGU 13-17 to be presented. We would also like recognise PetroHawk and St Marys for allowing their cores (from wells Elm Grove Plantation-63 and Johnson Trust 1-2H, respectively) to be sampled for these analyses and for permission to utilise their cores and to present these results. Finally, we are grateful to Chemostrat for allowing us the time and providing the support needed to prepare the article.

References

Donovan, A., 2010. The sequence stratigraphy family tree: understanding the portfolio of sequence methodologies. In: Ratcliffe, K.T. and Zaitlin B.A. (eds) Application of Modern Stratigraphic Techniques: Theory and Case Histories. SEPM Special Publication No. 94 p. 5-33.

Embry, A.F. 2010. Correlation siliciclastic successions with sequence stratigraphy. . In: Ratcliffe, K.T. and Zaitlin B.A. (eds) Application of Modern Stratigraphic Techniques: Theory and Case Histories. SEPM Special Publication No. 94 p. 5-33.

Jenkyns, H.C. 2010. Geochemistry of oceanic anoxic events. *Geochemistry Geophysics Geosystems*, v. 7, p.1-30.

Negri, A., Ferretti, A., Wagner, T. and Meyers, P.A. 2009. Organic-carbon-rich sediments through the Phanerozoic; processes, progress, and perspectives. *Palaeogeography, Palaeoclimatology, Palaeoecology*, v. 273, p. 302-328.

Paktunc, A.D. 2001. MODAN; a computer program for estimating mineral quantities based on bulk composition; Windows version. *Computers & Geosciences*, v. 27, p. 883-886.

Pearce, T.J., Wray, D.S., Ratcliffe, K.T., Wright, D.K. and Moscarello, A. 2005. Chemostratigraphy of the Upper Carboniferous Schooner formation, southern North Sea. *Carboniferous hydrocarbon geology: the southern North Sea and surrounding onshore areas*. In: Collinson, J.D., Evans, D.J., Holliday, D.W. and Jones N.S. (eds) *Carboniferous hydrocarbon geology: the*

southern North Sea and surrounding onshore areas. *Yorkshire Geological Society, Occasional Publications, Series, 7*, p. 147-64.

Ratcliffe, K.T., Wright, A.M., Montgomery, P., Palfrey, A., Vonk, A., Vermeulen, J. and Barrett, M. 2010. Application of chemostratigraphy to the Mungaroo formation, the Gorgon Field, offshore Northwest Australia. *APPEA Journal 2010 50th Anniversary Issue* p. 371 – 385.

Rosen, O.M., Abbyasov, A.A.; Tipper, J.C. 2004. MINLITH; an experience-based algorithm for estimating the likely mineralogical compositions of sedimentary rocks from bulk chemical analyses. *Computers & Geosciences*, v. 30, p. 647-661.

Schlanger, S.O. and Jenkyns, H.C. 1976. Cretaceous oceanic anoxic events: causes and

consequences. *Geol. Mijnb.*, v. 55, p. 179-194.

Tribouillard, N., Algeo, T., Lyons, T.W. and Riboulleau, A. 2006. Trace metals as paleoredox and paleoproductivity proxies; an update 2006. *Chemical Geology*, v. 232, p. 12-32.

Tribouillard, N., Bout-Roumazeilles, V., Algeo, T., Lyons, T.W.; Sionneau, T., Montero-Serrano, J.C., Riboulleau, A. and Baudin, F. 2008. Paleodepositional conditions in the Orca Basin as inferred from organic matter and trace metal contents. *Marine Geology*, v. 254, p. 62-72.

Turgeon, S. and Brumsack. H.J. 2006. Anoxic vs. dysoxic events reflected in sediment geochemistry during the Cenomanian–Turonian Boundary Event (Cretaceous) in the Umbria–Marche Basin of central Italy. *Chemical Geology* v. 234 p. 321-339. ■

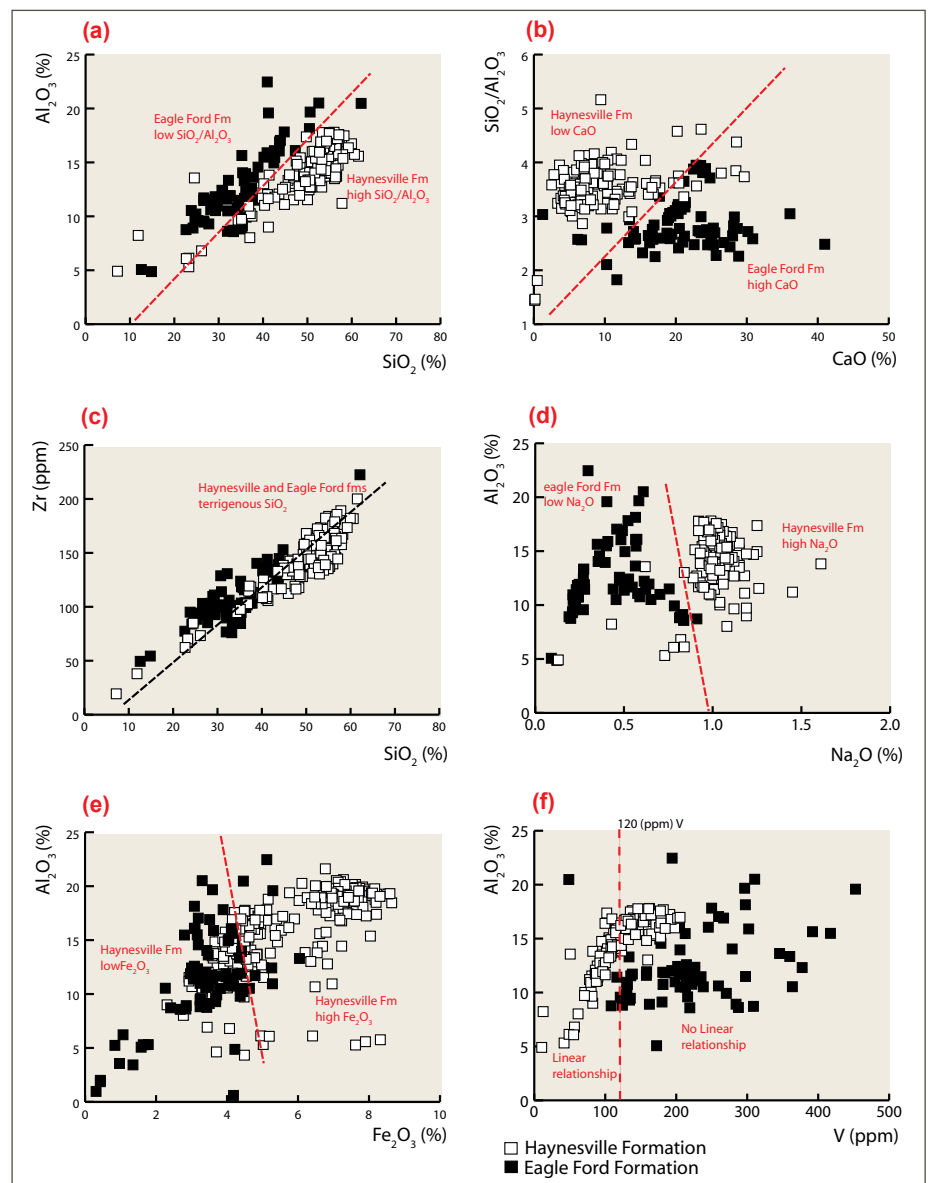


Figure 7. A-F: Cross plots of selected elements displayed for datasets from Haynesville (white squares) and Eagle Ford (black squares) formations.